CIVIL ENGINEERING JOURNAL

Article no. 11

THE CIVIL ENGINEERING JOURNAL 2-2025

REBAR-CONCRETE DEBONDING EFFECT ON THE SEISMIC PERFORMANCE OF REINFORCED CONCRETE SHEAR WALLS: AN EXPERIMENTAL STUDY

Afshin Hossein Sharifzadeh[1] and Saeed Tariverdilo[2]

1. *Department of Engineering, Faculty of Civil Engineering, Salmas Branch, Islamic Azad University, Salmas, Iran*
2. *University of Urmia, Faculty of Civil Engineering, Urmia, Iran; s.tariverdilo@urmia.ac.ir*

Received: *12.08.2024*

Received in revised form: *01.01.2025*

Accepted: *22.05.2025*

ABSTRACT

Diverse criteria are taken for seismic design of shear walls due to their buckling failure in various regulations. Despite extensive studies on the topic, no practical mechanism has been widely adopted to effectively mitigate out-of-plane buckling in reinforced concrete shear walls. This study presents a novel approach to address this issue by experimentally investigating the effect of rebar-concrete debonding on the seismic performance of boundary elements in shear walls with minimum reinforcement. Plastic sleeves, applied to rebar at varying lengths (80 mm, 150 mm, and 220 mm), were used to induce debonding and thus modify the stress transfer mechanisms and crack propagation within the concrete. Five experimental samples of shear wall boundary element were designed and constructed with minimum reinforcement. Samples were subjected to non-uniform cyclic loading to study rebar debonding effect on crack distribution, rebar strain, and out-of-plane instability in boundary element. The results indicate that debonding leads to a reduction in the lateral stiffness of the boundary elements, postponing rebar buckling, and also provides a 12% enhancement in the tensile capacity of the rebar. Findings illustrate rebar-concrete debonding results in a reduction in lateral stiffness of boundary element. Similarly, comparing to a debonding free element, buckling member occurs at more minimal strains. It is also revealed that to prevent buckling, larger dimensions are required for sleeved sample. Moreover, robust evidence proved that increasing rebar debonding length enlarges crack width near sleeves, while sleeve length does not affect the first buckling or axial length of samples. This study provides a practical and innovative mechanism for addressing buckling challenges in minimum-reinforcement boundary elements, contributing to safer and more efficient structural design practices.

KEYWORDS

Boundary elements, Out-of-plane buckling, Rebar debonding, Reinforcement fracture, Shear walls

INTRODUCTION

An overriding damage can occur as a result of failure in considering the mechanical forces' effect [1-4]. Accordingly, part of the energy, such as earthquakes and wind, imposed on the structure via external factors must be dissipated with minimal damage in a safe manner through plastic

deformation of different members. Such proceeding prevents the structure from instability against loads. Furthermore, innumerable concrete structures are mostly torn down and rebuilt due to unpermitted steady-state deformations and high costs of post-earthquake reconstruction. Distinct mechanisms can be taken to use up a large bulk of exerted energy on the structures' principal members. Hitherto, in recent years, dozen studies have exclusively addressed the performance of reinforced, strengthened concrete shear walls [5-7].

Cook et al. [8] examined failure causes in shear walls under 2010 Chilean earthquake and detected an identical failure in walls. In such type, crack concentration and rebar fracture were observed. According to ACI regulations, the plastic joint length should be approximately half the length of the wall. However, in this study, the minimum length was set to two to three times the wall thickness, which is considered minimal. Henceforth, insufficient plastic deformation capacity leads to insufficient ductility and finally minimum deformations under a seismic load arise reinforcement fracture. Previous studies have extensively investigated the behavior of reinforced concrete elements under seismic loading, particularly focusing on structures with minimum reinforcement. Hoult et al. [9] analyzed the seismic performance of U-shaped shear walls with less than 0.5% longitudinal reinforcement ratio and observed that strain concentration in the reinforcement tends to localize in a single crack, often leading to rebar fracture. This finding highlights the susceptibility of minimum-reinforced shear walls to failure due to inadequate strain distribution, emphasizing the need for strategies to mitigate such risks. Fantili et al. [10] empirically examined the effect of reinforcement diameter on the behavior of concrete beams with minimum reinforcement, demonstrating that larger reinforcement diameters influence crack propagation and strain distribution. These results underline the critical role of reinforcement characteristics in governing the performance of concrete elements under loading. Han et al. [11] surveyed the effect of boundary element details on seismic deformation of shear walls. In this research, shear walls with different reinforcement conditions and boundary element shapes were examined. It achieved conclusive findings revealing that the first flexural crack appears at a relative displacement of 0.17%–0.25% in the lower part of the boundary element. If steel tensile strength at initial crack location (cracked section) is higher than that of concrete (un-cracked section), flexural cracks could develop. Henceforth, boundary reinforcement is concentrated along the wall edges (boundary element). Khalfallah [12] performed a crack analysis on reinforced concrete tensile members. The study concluded post-cracking behavior of reinforced concrete member depends on parameters such as concrete strength, development length for reinforcement, concrete-rebar connection, and distance between rebars. Chrysanidis et al. [13] discussed tensile strain effect on lateral buckling of wall boundary element. Their study revealed instability and lateral buckling increase in tensile strain of rebar of shear wall boundary element.

Rebar-concrete bond effect on longitudinal reinforcement strain distribution could be considered as other effective parameter affecting concrete shear walls behavior [14-16]. Such issue constituted a research topic for numerical researchers in this domain [17-19]. Fantili et al. [20] studied members' bond-slip behavior under tension at cracked section. Findings demonstrated tensile force exerted on crack location member is carried by rebar, and so applied force to concrete is via bonding force. Muhamad et al. [21] experimentally studied load-slip relationship of tensile reinforcement in reinforced concrete members. In this study, flexural members' deformation divided into continuous and non-continuous (deformation). Hong and Park [22] investigated rebar-concrete bond-slip relationship and provided a new behavioral model for slip-shear stress along the interface between rebar and concrete. In another empirical study, Tastani et al. [23] examined rebar indentation area effect on strain penetration and rebar-concrete debonding. This study concludes strain penetration will reduce through an increase in indentation surface area. Naghipour et al. [24] empirically evaluated bonding stress and rebar slip behavior in concrete under reciprocating static loading as well as concrete confinement effect. Guizani et al. [25] examined bond-slip behavior via previous models to consider stirrup placement effect in medium-ductility reinforced concrete structures. The study observed stirrup confinement increase along bond strength between rebar and concrete. Bao et al. [26] introduced a method to prevent and reduce progressive collapse risk in reinforced concrete

structures. In this method, rebar-concrete debonding (sleeving) was applied to improve ductility around 30%. This phenomenon also converted strain concentration in a cracked expansion in beam into strain propagation along sleeve and hence delayed fracture. Hussein et al. [27] studied bonding and debonding effect of reinforced rebar in concrete structures' vibration behavior with normal and high-strength concrete. The study displayed rebar-concrete debonding could increase beams ductility. Opabola et al. [28] investigated slip and shear deformations influence on the elastic response of RC components. The study achieved reliable evidences in damage reduction as well as absorption increase of seismic energy. Furthermore, findings revealed diagonal reinforcement strain uniformity as well as its independency from flexural stress. Henceforth, diagonal deformation increases and rebar usage reduction emerge.

The seismic performance of reinforced concrete shear walls is critical for the safety and resilience of structures in earthquake-prone regions. Despite advancements in design approaches, one persistent challenge is the out-of-plane buckling of boundary elements, which undermines the structural integrity of shear walls. Existing studies have extensively investigated factors influencing buckling and crack propagation in these elements. However, these studies have largely focused on traditional reinforcement strategies without exploring innovative mechanisms to mitigate buckling in structures with minimum reinforcement. This research aims to address this gap by introducing and experimentally evaluating the effects of rebar-concrete debonding through the use of plastic sleeves. By strategically isolating sections of the rebar, the study investigates how this technique impacts strain distribution, crack behavior, and buckling in boundary elements under seismic loading. The findings of this research have the potential to influence industry practices by providing a practical solution for improving the seismic performance of reinforced concrete shear walls, particularly in cost-sensitive projects requiring minimum reinforcement. Moreover, the results could inform future updates to seismic design codes and regulations, promoting the adoption of rebar-concrete debonding as a viable strategy for mitigating buckling and enhancing structural safety.

Walls with minimum reinforcement ratios are more prone to instability because they lack the necessary resistance to buckling and stress distribution. The minimal reinforcement leads to a higher concentration of stresses at crack locations, reduced ductility, and early fracture of reinforcement. These factors make such walls more vulnerable to failure under seismic loading. This research focuses on improving the performance of these walls by investigating the effect of rebar-concrete debonding, which can potentially reduce buckling and enhance stability in walls with minimal reinforcement. Almost all literature review revealed a high demand for tensile rebar strain at crack location. It is also emerged that tensile rebar strain at crack location is the momentous failure in shear walls with minimum longitudinal reinforcement ratio which ultimately leads them to rebar fracture. On the other hand, findings of the current study demonstrate method of debonding, elimination or concrete-rebar bond reduction could increase beams and columns ductility. Accordingly, ultimate goal of the present study is to examine experimental distribution of longitudinal rebar strain in boundary element of shear walls via minimum reinforcement. As a pioneer study in this field, it also considers the effect of such process on buckling stability of shear walls considering local rebar-concrete debonding (sleeving). Such a consequential issue is conducted taking several experimental tests on various samples for boundary element of reinforced concrete shear walls. The firm claim is that changes in tensile force at the base of shear wall are smaller than the wall height due to low bending moment gradient. Henceforth, considering this hypothesis, a prismatic element under tension at two ends can be applied to model shear wall boundary element. Accordingly, four different samples without rebar debonding were subjected to cyclic loading followed by three samples with different sleeve lengths. Then, rebar strain distribution and failure mode, including cracks and buckling distribution, were examined to evaluate sleeving effect on seismic behavior of shear wall boundary element.

METHODS

Initially, three rebar debonding free samples were subjected to monotonic and cyclic loading to evaluate sleeving effect on seismic behavior of shear wall. Then, three samples with different sleeve lengths were subjected to cyclic loading, and strain distribution in rebar and failure mode, including crack distribution and buckling, were studied. Steps for selection, samples' dimensions and methodology are as follows: Selection of sample's dimensions, Selection of rebar and concrete strength, Conduction of Rockwell tests on rebars prior than principal experiment, Design of laboratory setup for sample testing, Selection of loading protocol, Placement and testing of samples, and registration of experimental data, Destruction of samples after their loading and Rockwell tests.

Seven prismatic samples with section dimensions of 150 mm × 150 mm and a length of 1000 mm are opted to evaluate seismic behavior of shear wall boundary element. Fig. 1 displays the geometric properties of samples under study. Two of samples (BM2 and BM3) were sleeveless and subjected to cyclic loading as reference samples. Moreover, three sleeved samples (DC1, DC2, and DC3) were subjected to cyclic loading. The dimension selection and sample preparation were conducted considering two issues; the operating limits of testing device (motion range of the jack) and ACI318R-14 regulations [29] in such a way that an element does not undergo overall buckling during loading. Concrete foundations with dimensions of 600 mm × 450 mm × 150 mm were applied to meet two purposes: to connect prismatic piece to loading jack and laboratory rigid floor and to provide development length of reinforcement. Fig. 1b illustrates the experimental setup prepared at Infrastructure Research Center at Urmia University. Furthermore, having observed the minimum vertical reinforcement ratio in shear wall based on ACI318R-14, the study applied indented type 10T longitudinal reinforcement. It should be nominated that reinforcement ratio of cross section was higher than that recommended by ACI318R-14. Plain 6T rebars placed at distances of 75 mm were used to concrete confinement at element core.

The experimental dimensions and parameters were carefully chosen to represent realistic scenarios encountered in reinforced concrete shear walls with minimum reinforcement while allowing for controlled laboratory testing. The test specimens were designed to reflect typical dimensions and reinforcement ratios used in real-world reinforced concrete shear walls, with a height-to-width ratio of 2.5:1 to simulate slender boundary elements. Due to laboratory constraints, the specimens were scaled to manageable sizes while maintaining realistic proportions, ensuring the relevance of the experimental results to actual field conditions. The longitudinal reinforcement ratio of 0.351% was selected to align with the minimum reinforcement requirements specified in seismic design codes and to facilitate comparison with similar studies.

The sleeve lengths of 80 mm, 150 mm, and 220 mm were selected to represent varying degrees of rebar debonding commonly encountered in construction. The 80 mm length simulates minimal debonding, which might be used in cases where only slight improvements to strain distribution are needed. The 150 mm length corresponds to moderate debonding, reflecting a common approach in seismic design to balance reinforcement efficiency and performance. Finally, the 220 mm length represents a more substantial debonding, suitable for high-performance applications where significant strain redistribution is necessary to prevent premature failure. These lengths were chosen based on practical considerations and typical construction practices, ensuring that the experimental results are relevant to real-world applications in reinforced concrete shear wall design. The choice of sleeving lengths (80 mm, 150 mm, and 220 mm) was informed by preliminary trials and literature observations indicating that localized detachment can influence strain distribution and crack patterns in reinforced concrete elements. These lengths were chosen to cover a range of detachment effects, from minimal to more significant, enabling a comprehensive analysis of the technique's impact. By grounding the experimental setup in established research while introducing innovative parameters, such as the sleeving mechanism, this methodology ensures both relevance to practical applications and the ability to draw meaningful comparisons with prior studies.

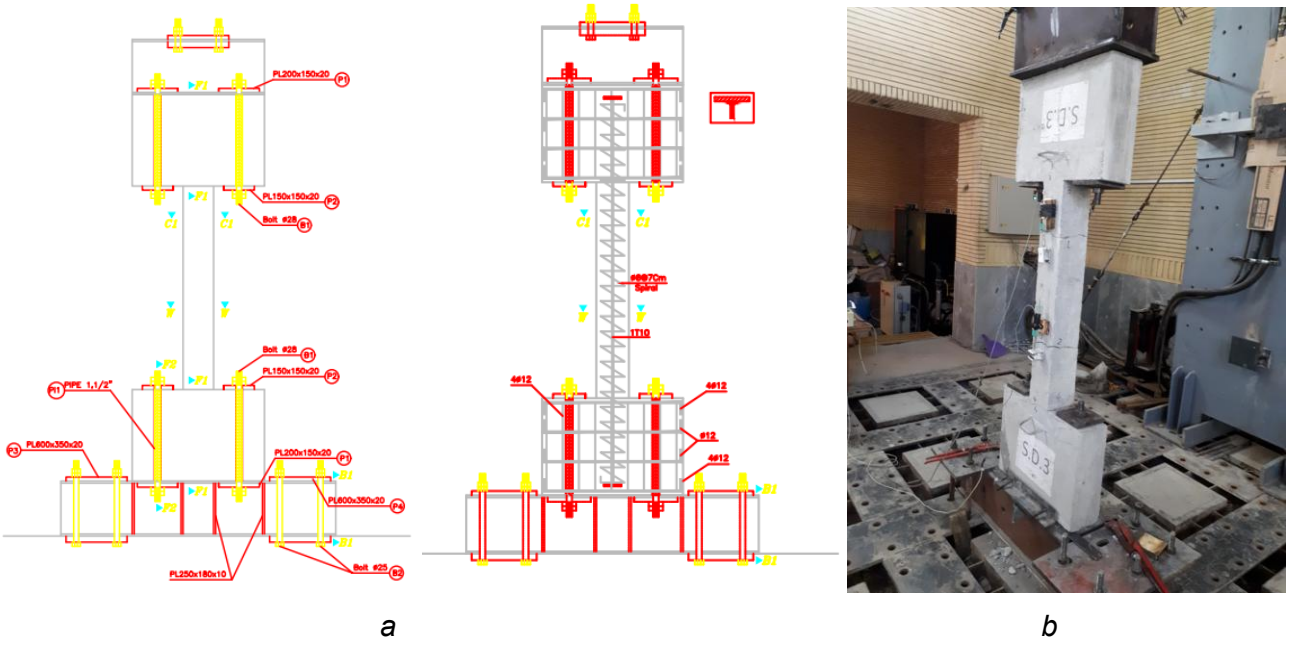

a *b*

c *d*

Fig. 1 - (a) Geometric properties of samples under study; (b) experimental setup and method of samples installing; (c) rebar sleeving method; (d) reinforcement and construction details of concrete boundary element before concrete placement

To investigate the effect of rebar separation on the seismic behavior of the shear wall boundary element and the stress distribution in the longitudinal rebar, three laboratory specimens were prepared. A plastic hose, matching the diameter of the rebar, was used as the sheath to create debonding. The sheaths were placed at the mid-height of the specimens with lengths of 80 mm, 150 mm, and 220 mm. Before positioning the sheaths, the rebars were greased at the specified locations to minimize interaction between the rebar and the sheath body, ensuring effective debonding at the designated lengths. The plastic sleeves were subsequently and securely positioned at specified locations on the rebar, as shown in Figure 1c. These sleeves were carefully placed to ensure uniform debonding along the reinforcement. Following the installation of the sleeves, all three specimens were subjected to seismic loading according to a standardized loading protocol. This protocol was designed to replicate realistic seismic conditions and assess the performance of the specimens under cyclic loading, ensuring consistency in the testing procedure across all samples. The summary of the specifications of the samples and the load application method employed in the experimental study is shown in Table 1.

Tab. 1 - A summary of the specifications of the samples and the method of load application utilized in the experimental study

Sample No.	Loading Type	Lateral Reinforcement	Longitudinal Reinforcement	Percentage of Reinforcement (%)	Sleeve Length (mm)
BM2	Monotonic	φ6@70 mm	T10	0.351	--
BM3	Monotonic	φ6@70 mm	T10	0.351	--
BC1	Cyclic	φ6@70 mm	T10	0.351	--
BC2	Cyclic	φ6@70 mm	T10	0.351	--
DC1	Cyclic	φ6@70 mm	T10	0.351	80
DC2	Cyclic	φ6@70 mm	T10	0.351	160
DC3	Cyclic	φ6@70 mm	T10	0.351	240

Direct tension tests were conducted on the rebars, as outlined in reference [30], to evaluate their tensile strength and deformation characteristics under controlled conditions. Corresponding stress-strain curves of rebar is displayed in Figure 2a. Direct tension test findings demonstrate ISIRI3132 reinforcement is S400 grade and exactly meets tensile strength requirements and elongation of reinforcement. Given sample dimensions and concrete coating thickness on lateral reinforcement, the study used C30 concrete to prepare samples both via a suitable mix design selection and maximum grain size observation. The characteristic compressive strength in 28-day concrete cylinder samples with dimensions of 100×300 reaches 30 MPa. Figure 2b depicts compressive test of concrete cylindrical test.

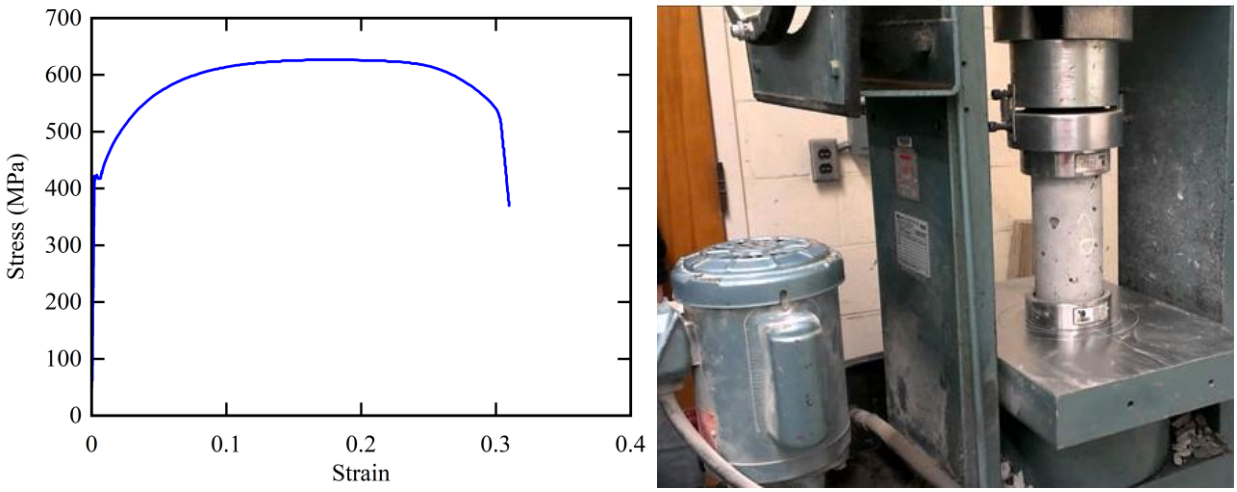

a *b*

Fig. 2 - (a) Stress-strain curve of rebar; (b) Determination of compressive strength of the concrete

Wall fracture in minimum longitudinal reinforced sheer walls is substantially controlled due to tensile load on boundary elements. Henceforth, boundary elements are not required to endure a serious compressive load. An asymmetric loading protocol, similar to ACI 355.2 protocol [31], was considered for cyclic loading. Such loading protocol comprised of symmetric cycles of increasing axial strain around 0.003. This figure achieves after continuously stable increase is notified in tensile loading range, while compressive strain ends at 0.003. Applied cyclic loading protocol has been illustrated in Figure 3. The protocol consists of asymmetrical displacement cycles with increasing amplitudes to simulate seismic loading conditions. The initial cycles represent lower displacement values to assess the elastic behavior of the specimens, while subsequent cycles introduce larger displacements to evaluate the capacity for energy dissipation, crack propagation, and eventual failure modes under realistic seismic conditions.

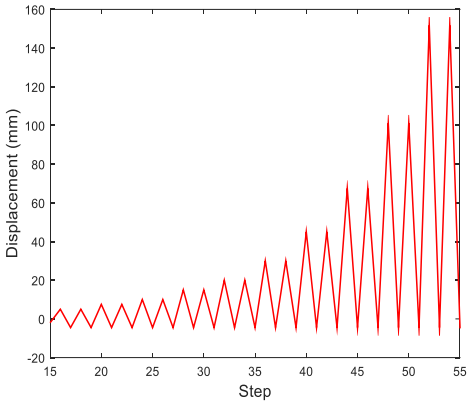

Fig. 3 - Applied loading protocol in large-displacement asymmetrical loading tests. The graph shows the cyclic loading sequence applied to the shear wall boundary elements during the experimental tests.

Since the expansion of cracks in the boundary element of the shear wall has led to a decrease in lateral stiffness, so that the buckling of the boundary element can occur before the buckling and rupture of the longitudinal bar. In this regard, Dashti et al. [32] realized the relationship between the horizontal displacement of the middle of the wall and the buckling of the wall and presented the equation (1) relating the lateral displacement with the reinforcement ratio.

$$\xi = \frac{\delta}{b} \le 0.5\left(1 + 2.35\frac{\rho f_y}{f_c'} - \sqrt{5.53\left(\frac{\rho f_y}{f_c'}\right)^2 + 4.70\frac{\rho f_y}{f_c'}}\right) \quad (1)$$

in which δ is the lateral displacement of the middle of the element, b is the section dimension, and ρ is the reinforcement ratio in the border element of the shear wall. The average critical strain caused by plate buckling for a sample with one layer of reinforcement can be estimated according to the following equation.

$$\varepsilon_{cr} = 4\left(\frac{b}{l_o}\right)^2 \xi_{cr} \quad (2)$$

RESULTS

This section addresses findings for sleeveless samples BC1 and BC2 (reference samples), sleeved samples DC1, DC2, and DC3 based on cyclic loading test via loading protocol. Loading test was continued until the rebar fracture occurs.

The BC1 sample was subjected to cyclic loading based on the defined loading protocol to study the seismic behavior of boundary elements in shear walls with minimum reinforcement. The load-displacement curve is displayed in Figure 4. In subsequent cycles, cracks appeared abruptly as the load force increased (e.g., cracks 3 and 5) and were closely spaced (as shown in Figure 4b). At these locations, failure initiated with concrete crushing followed by longitudinal reinforcement buckling between two cracks. A further increase in load led to fatigue fracture of the reinforcing rebar, with the ultimate tensile deformation upon failure reaching approximately 88 mm. At these locations, failure initiated with crushing of concrete followed by buckling of longitudinal reinforcement between two cracks. Further increase in load leads to fatigue fracture of reinforcing rebar. Maximum or ultimate tensile deformation upon failure was about 88 mm.

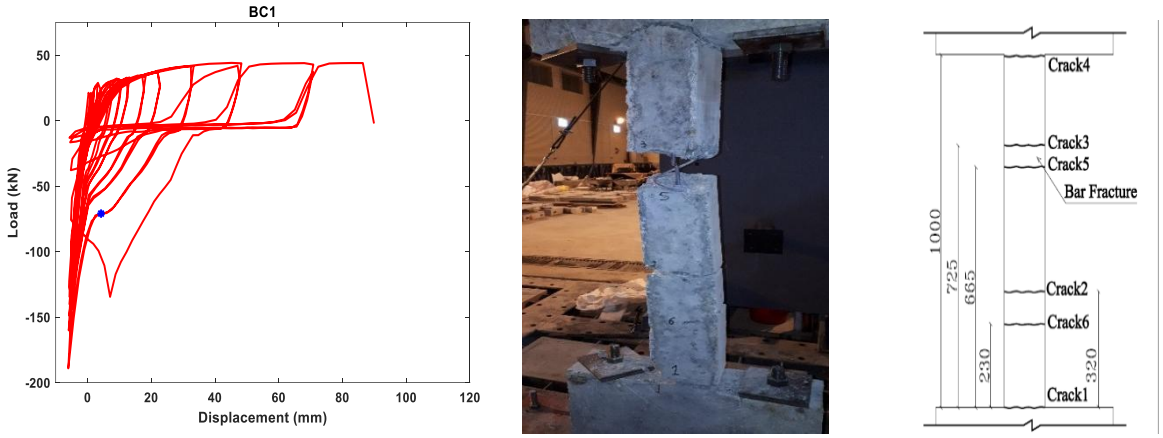

a b c

Fig. 4 - (a) Load-displacement graph under cyclic loading for BC1 sample. This graph shows the relationship between the applied load and displacement, with the initial steep slope indicating elastic behavior and the flattening of the curve reflecting stiffness reduction due to crack formation. (b) Crack geometry showing the distribution and locations of cracks. (c) Crack shape highlighting the morphology of cracks, emphasizing the primary cracks leading to rebar fracture.

Similar to other samples, in BC2, the first crack occurred in fifth cycle at distance 325 mm from joint region along element and foundation via applied cyclic loading. Additional cyclic loading leads to second crack at joint region along element and upper foundation. Then, further cyclic loading makes the third and fourth cracks in ninth and tenth cycles at distance 710 mm from joint region along element and footing; and element and foundation, respectively. Figure 5a displays load-elongation graph of sample under cyclic loading. Also, Figure 5 illustrates crack distribution along sample. Although failure location of Crack 3 initiated in concrete crushing and global buckling forms, ultimate failure happened as rebar fracture at the first crack location (Crack 1).

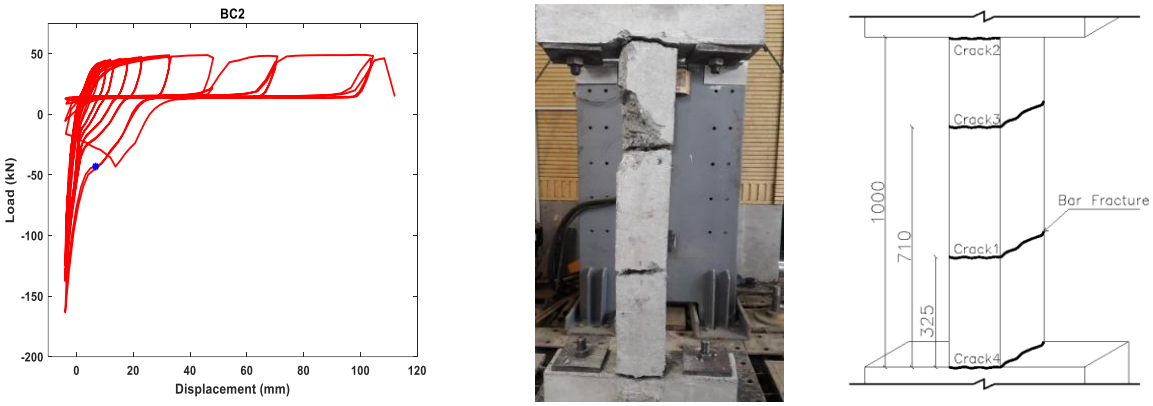

a b c

Fig. 5 - (a) Load-displacement graph under cyclic loading for BC2 sample, showing initial elasticity and stiffness reduction as cracks form. (b) Crack geometry and (c) crack shape, highlighting crack distribution and key fractures leading to rebar failure.

In DC1, with rebar-concrete debonding sleeves in the middle of height with a length 80 mm, the first crack occurred with applied cyclic loading at joint region along element and foundation. Figure 6 displays schematic diagram of failure and load-displacement graph. According to Figure 6, as load increases in subsequent cycles, three other cracks appeared at distances of 80 mm, 210 mm, and 390 mm. These cracks were mainly concentrated in the lower part of sample. As shown in Figure 6, with further loading, buckling failure occurs during 20th cycle. After Crack 5 appears at joint

region along sample and foundation, another crushing failure occurs at Crack 3 during 22nd cycle. The ultimate failure happened as rebar fracture in Crack 2 under the sleeve.

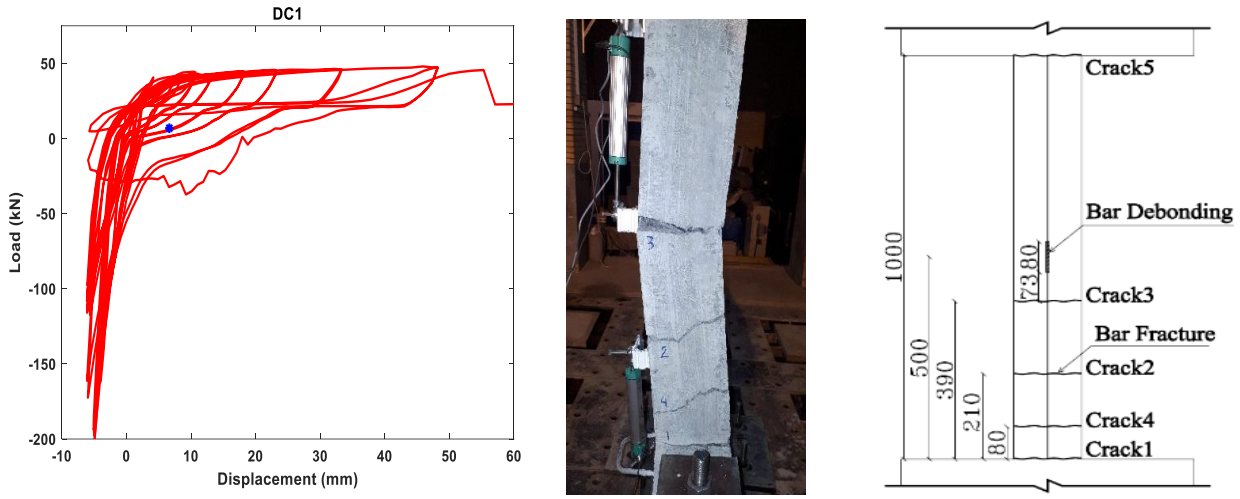

a b c

Fig. 6 - (a) Load-displacement graph under cyclic loading for DC1 sample, showing the load-displacement relationship with stiffness reduction as cracks form. (b) Crack geometry and (c) crack shape, highlighting the distribution and key fractures leading to rebar failure.

In DC2, with the rebar-concrete debonding sleeves in the middle of height with a length 60 mm, as shown in Figure 7, the first crack occurred at distance 385 mm from joint region along element and foundation. Increasing load produces crack width increase to 16 mm under tension during 23rd cycle. In next cycle, concrete crushing at horizontal crack and vertical crack propagation along rebar appeared. The ultimate failure occurred without any new cracks as rebar fracture at Crack 1 under sleeve. Absence of any crack propagation and initiation along sample produced no lateral buckling. Comparing to other samples, absence of initiation of secondary cracks in DC2 lead to overall deformation of sample at minimum level. Henceforth, rebar fracture occurred at low cycles.

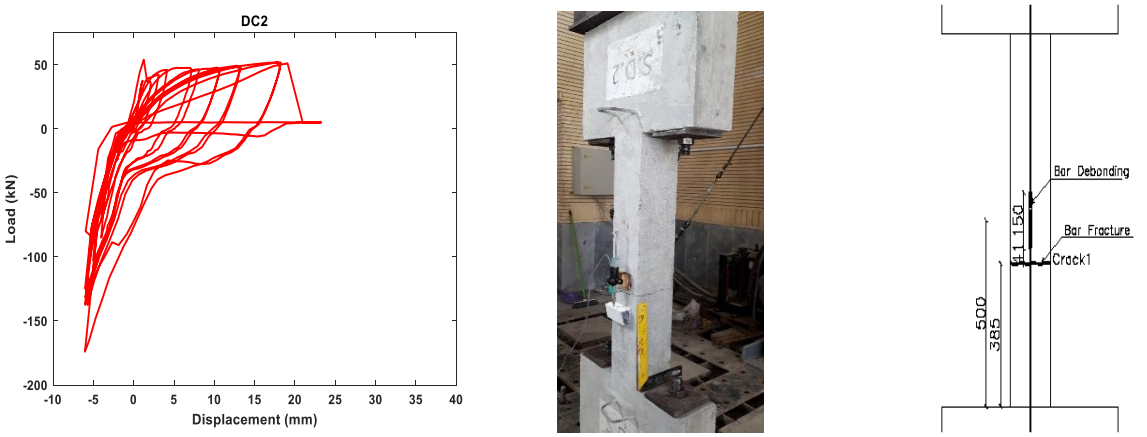

a b c

Fig. 7 - (a) Load-displacement graph under cyclic loading for DC2 sample, showing the load-displacement relationship with stiffness reduction as cracks form. (b) Crack geometry and (c) crack shape, highlighting the distribution and key fractures leading to rebar failure.

The occurrence of early fractures in some samples highlights the complex interplay between the debonding mechanism, crack patterns, and strain distribution. While the sleeving mechanism improves fracture strain in certain scenarios, it also introduces new stress concentrations near the sleeve boundaries. These observations suggest that careful consideration must be given to the

length and placement of the sleeves to optimize their effectiveness. In seismic design, this underscores the need for a balance between achieving strain redistribution and avoiding localized vulnerabilities that could compromise the overall performance of the boundary element. The ultimate failure occurred without any new cracks as rebar fracture at Crack 1 under sleeve. Absence of any crack propagation and initiation along sample produced no lateral buckling. Comparing to other samples, absence of initiation of secondary cracks in DC2 lead to overall deformation of sample at minimum level. Henceforth, rebar fracture occurred at low cycles.

In DC3, with the rebar-concrete debonding sleeves in the middle of height with a length 220 mm, the first crack occurred in the third cycle at distance 280 mm from joint region along element and foundation. Load-displacement graph and crack geometry of this sample are displayed in Figure 8. Increasing load produced second crack 5th cycle at distance 785 mm from joint region along element and foundation. As illustrated in Figure 7, the third and fourth cracks occurred in 9th and 11th cycles, respectively, at two ends of elements at joint region with foundation. The element failure in 26th cycle occurred as global buckling (instability), and cracks along longitudinal reinforcement were observed during 36th cycle at Cracks 1 and 2 along concrete weight coating. Finally, rebar fractured at Crack 1 during 39th cycle in a way that widths of Cracks 1 to 4 were 6 mm, 11 mm, 26 mm, and 35 mm, respectively. Similar to reference samples (BC1 and BC2) and sleeved sample (DC1), in the present sample, failure occurred as out-of-plane buckling with concrete crushing at crack location before rebar fracture. Findings for Rockwell are illustrated in Figure 9.

The sleeve length significantly influences the crack width in shear walls with rebar debonding. As the sleeve length increases, the debonding effect becomes more pronounced, redistributing strain and leading to wider cracks near the sleeve. This can enhance energy dissipation and strain redistribution, improving the seismic performance and ductility of the structure. However, wider cracks also weaken the bond between the concrete and rebar, reducing the concrete's ability to transfer forces effectively. This can lead to localized failure in the concrete, potentially compromising the wall's overall integrity. Therefore, sleeve length must be carefully balanced to optimize seismic performance while minimizing the risk of localized damage from excessive crack widths.

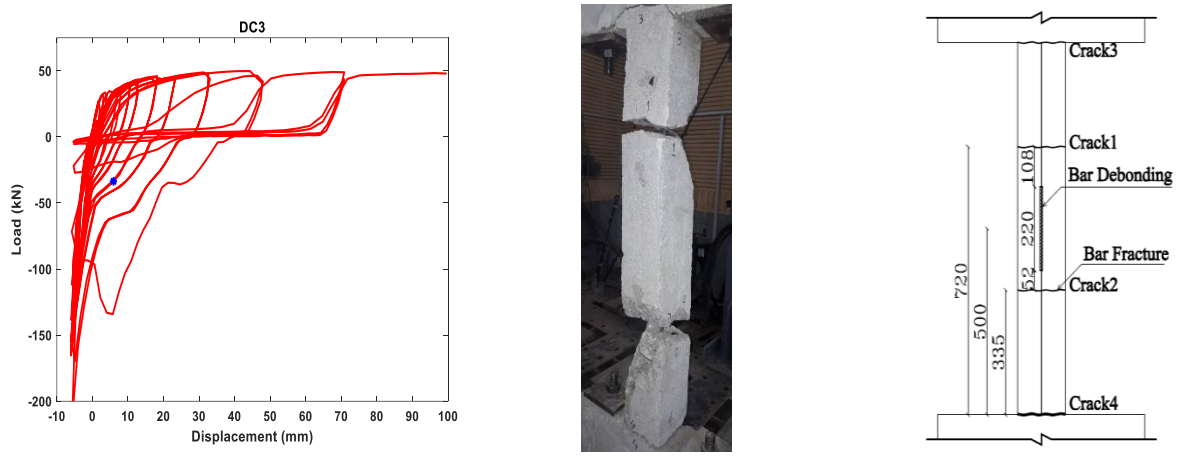

a *b* *c*

Fig. 8 - (a) Load-displacement graph under cyclic loading for DC3 sample, showing the load-displacement relationship with stiffness reduction as cracks form. (b) Crack geometry and (c) crack shape, highlighting the distribution and key fractures leading to rebar failure.

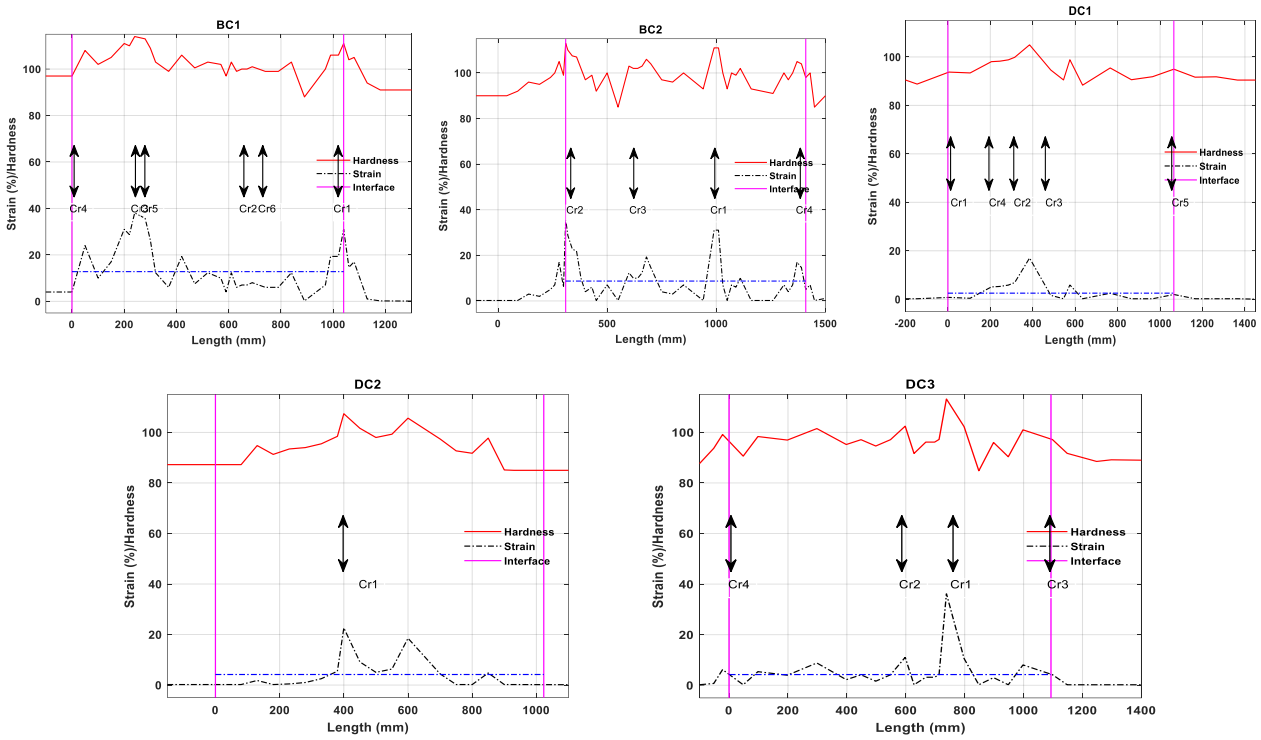

Fig. 9 - Strain distribution along the reinforcement in various samples, illustrating the variation in strain at different locations along the reinforcement for each sample.

For cyclic loading tests, the cracking pattern is highly similar to observed monotonic loading. Because of strain penetration into foundation, in samples subjected to cyclic loading, rebar fracture occurred for both BM2 and BM3 at joint region along member and foundation element. In addition, out-of-plane buckling is an overriding reason for change in rebar fracture location. Out-of-plane buckling is also a substantial reason for rebar fracture in the middle region. Nevertheless, numbers and patterns of cracks in sleeved samples (DC1 and DC3) are diverse and various, out-of-plane buckling in both samples occurred at the average strain. Such evidence confirms the relationship between buckling and average axial deformation. Since crack widths do not represent strain distribution before buckling, henceforth, no analysis could be practiced on uniform elongation of such samples. Subsequently, rebar-concrete debonding effect on boundary element's seismic behavior in shear wall with minimum reinforcement is investigated via two perspectives:

1) Impact of longitudinal reinforcement strain on buckling instability
2) Impact of longitudinal reinforcement strain on drift

Table 2 summarizes findings for cracking in sleeved and sleeveless samples under cyclic loading. It covers both buckling and corresponding state to rebar fracture. Based on demonstrated findings in Table 2 and also taking into account the average strain upon buckling for both sleeved and sleeveless samples, it is more likely to deduce that comparing to sleeveless samples, sleeved samples experience buckling at minimum strains. Furthermore, it can be claimed that sleeve length does not play a crucial role in buckling control of boundary element. The experimental results demonstrate that the fracture strain of the rebar increases from 0.088 in the case of no sheath to 0.098 when a sheath with a length of 240 mm is used. This represents a 12% improvement in the fracture strain of the rebar. This enhancement highlights the potential of the rebar-concrete debonding mechanism to improve the ductility and deformation capacity of reinforcement, thereby contributing to better seismic performance of shear wall boundary elements. With the weakening of the bond between the rebar and concrete near the sleeve, the ability of the concrete to transfer axial and shear forces to the reinforcement is diminished. This can result in premature rebar fracture or failure at the sleeve location, which could limit the wall's overall capacity to resist seismic forces.

Tab. 2 - Summary for cracking in different elements under study

Sample	Failure Mode	Crack Number and Width (mm)						Sample Elongation (mm)	Average Strain εsm1
		1	2	3	4	5	6		
BC1	Buckling	5	4	9*	7	7	-	32	0.032
	Rebar Fracture	20	19	14**	21	25	12	88	0.088
BC2	Buckling	10*	5	9	8	--	--	32	0.032
	Rebar Fracture	25	19**	22	18	--	--	84	0.084
DC1	Buckling	3	6*	5	4	--	--	18	0.018
	Rebar Fracture	7	24**	23	6	5	--	65	0.065
DC3	Buckling	5	7*	2	4	--	--	18	0.018
	Rebar Fracture	24	36**	6	32	--	--	98	0.098
*Maximum crack width upon initial buckling in sample **Rebar fracture									

One of the key applications of the strain distribution diagram along the element is to assess both the maximum local strain within the reinforcement and the uniform strain distribution along the entire length of the element. This analysis is crucial for understanding the strain variation and identifying potential points of failure within the reinforcement during loading. The uniform strain is calculated by dividing the total elongation, which is derived from summing all local strains along the reinforcement, by the total length of the reinforcement. The values for both the uniform and maximum strains, as measured in the sleeved and sleeveless samples, are presented in Table 3. It is totally worthwhile to notify that maximum strain values obtained are not caused only by axial deformation. They are also dramatically affected by bending deformation. As the sleeve length increases, the debonding effect becomes more pronounced, leading to a concentration of strain near the sleeve edges. This can cause localized concrete cracking or spalling, reducing the concrete's ability to transfer forces effectively and compromising the overall structural integrity.

The observed instability in sleeved samples at lower strains can be attributed to stress concentrations near the edges of the sleeves. The debonding effect, induced by the plastic sleeves, weakens the bond between the rebar and concrete, leading to a redistribution of strain along the reinforcement. This redistribution causes localized stress concentrations near the sleeve edges, which can initiate buckling or other forms of instability at lower strains compared to unsleeved samples.

Tab. 3 - Elongation and Deformation Data Taken from Samples

Sample	Average Elongation (mm)	Average Strain *	Uniform Strain **	Maximum Strain **	Permissible Drift †	εcr‡	εcr
BC1	88	0.088	0.085	0.361	0.041	0.032	0.0176
BC2	84	0.084	0.087	0.357	0.031	0.032	0.0176
DC1	65	0.065	0.0251	0.170	0.023	0.018	0.0176
DC2	25	0.025	0.0418	0.226	0.009	---	0.0176
DC3	98	0.098	0.0423	0.382	0.035	0.018	0.0176
* Ratio of elongation to sample length ** Obtained via relationship between stiffness and strain. † Obtained via Dezhdar and Adebar's proposed method [33]. ‡ Tensile strain corresponding to first out-of-plane buckling.							

Figure 10 compares expected and actual drift capacity of samples. Such capacities are compared to rebar strain in various samples under study. Based on findings, regarding sleeved and sleeveless samples, there are sufficient evidences to deduce that an increase in sleeve length can somehow affect drift capacity of element. On the other hand, crack and strain concentration in DC2 brings about weak drift capacity. Henceforth, failure occurs as a result of rebar fracture at minimum deformations before buckling.

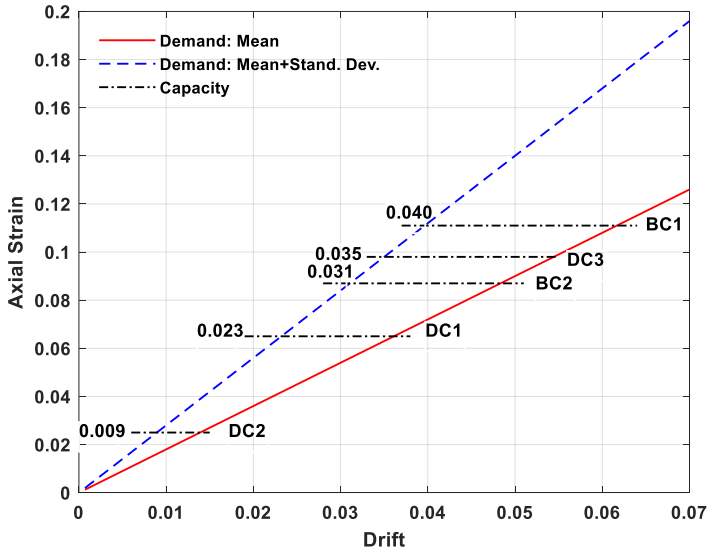

Fig. 10 - Comparison of expected and actual drift capacities of samples compared to rebar strain

The findings indicate that while rebar-concrete debonding can enhance strain distribution and delay buckling, improper implementation may lead to premature failure. These results suggest that design guidelines for implementing rebar debonding mechanisms should consider not only the benefits but also the potential risks of localized strain concentration. Future work could explore optimized sleeve geometries and material properties to mitigate these risks, thereby improving the seismic resilience of reinforced concrete shear walls. Building on these insights, our study hypothesizes that introducing a rebar-concrete detachment mechanism (via plastic sleeves) can address the strain concentration and improve strain distribution along the rebar. This approach aims to reduce the likelihood of localized fractures, as observed by Hoult et al. [9], and to optimize the behavior of the reinforcement, extending the principles identified by Fantili et al. [10] to the context of shear walls. By experimentally investigating this hypothesis, we seek to provide a novel mechanism for enhancing the seismic performance of minimum-reinforced boundary elements.

While rebar-concrete debonding offers significant benefits, such as improved strain redistribution and energy dissipation, it also introduces potential risks. The concentration of stress near the sleeve edges can cause localized concrete failure, reduce force transfer between the concrete and rebar, and increase the likelihood of premature rebar fracture or buckling. Therefore, the use of debonding must be carefully controlled to balance its seismic benefits with the risks of localized damage and reduced lateral stiffness. This study presents a novel investigation into the effect of rebar-concrete debonding in shear walls with minimum reinforcement, an area that has not been extensively studied in the literature. While previous research has focused on traditional reinforcement strategies, our findings provide new insights into the seismic performance of walls with minimum reinforcement, revealing both the benefits, such as improved strain redistribution, and the risks of localized failure due to stress concentrations near the sleeve edges.

Based on the findings of this study, several recommendations for updating seismic design guidelines are proposed. First, standardizing sleeve dimensions within a range of 80 mm to 220 mm would provide flexibility in addressing different levels of rebar debonding effects while maintaining structural integrity. Second, optimal sleeve placement should be considered, with sleeves placed at

mid-height or near critical regions of the shear wall to ensure effective strain redistribution and minimize stress concentrations. Finally, sleeve length and placement could be adjusted according to the seismic risk of the region. In areas with higher seismic activity, longer sleeves may be necessary to enhance strain redistribution, while in lower seismic risk regions, shorter sleeves could be more appropriate to achieve the desired performance without compromising the overall stability of the wall.

CONCLUSION

The present study experimentally investigated rebar debonding effects on boundary element's seismic performance in reinforced-concrete shear walls with minimum reinforcement. Thereupon, fully experimental tests were conducted on diverse samples applying asymmetric cyclic loading for both sleeved and sleeveless samples. Ultimately, evaluation developed at strain distribution along element and buckling of boundary element. Based on conducted experiments and analyses:

- Concrete-rebar debonding reduces the lateral stiffness of boundary element. Hence, compared to debonding free element, buckling occurs at minimum strains.
- Larger dimensions are required for sleeved sample to prevent buckling. For instance, under a longitudinal reinforcement ratio of 0.351%, the maximum tensile strain prior to buckling is approximately 0.02 for unsheathed specimens and 0.032 for sheathed specimens. These values are notably lower than the anticipated tensile strain capacity of the elements. Such values are less than expected tensile strain capacity for elements.
- Sleeved rebars experience cracks at distances 5φ to 7.5φ (φ is the diameter of the longitudinal rebar) from end of sleeve location. Cracks adjacent to sleeved length have the largest width. This crack is expected to release deformation along sleeve.
- The results indicate that the fracture strain of the rebar increases from 0.088 in specimens without a sheath to 0.098 in those utilizing a 240 mm-long sheath. This enhancement represents a 12% improvement in the fracture strain of the rebar.
- An increase in rebar debonding length increases the crack width near sleeving. Nevertheless, sleeving length does not affect first buckling of sample or axial elongation of samples.
- Rebar-concrete debonding using plastic sleeves offers a practical method to redistribute strain, delay buckling, and improve fracture strain capacity in reinforcement. This technique can enhance the seismic performance of shear walls in cost-sensitive, minimum-reinforcement projects. Proper sleeve length and placement are crucial to maximize benefits and minimize localized strain concentrations.
- The findings suggest the need for updated design guidelines to incorporate rebar debonding mechanisms. Recommendations should address sleeve dimensions, placement, and materials to encourage safer and more resilient seismic designs in reinforced concrete structures.

This study introduces a novel mechanism for mitigating out-of-plane buckling in shear wall boundary elements by leveraging rebar-concrete debonding. By selectively incorporating sleeving around the rebar, the study demonstrates the potential to improve strain distribution, increase fracture strain capacity, and delay buckling under seismic loading. This approach is particularly beneficial for structures with minimum reinforcement, where conventional methods may fail to prevent premature buckling. These findings provide a practical and cost-effective strategy for enhancing the seismic performance of reinforced concrete shear walls, offering a significant advancement over existing design methods.

The findings of this study have significant practical implications, especially for retrofit projects and cost-sensitive scenarios where minimum reinforcement is common. Rebar-concrete debonding provides a cost-effective method to improve seismic performance in both existing structures and new buildings, where budget constraints may limit the amount of reinforcement. This technique enhances energy dissipation and reduces the risk of premature buckling, offering a valuable solution for improving structural resilience without significant additional costs.

REFERENCES

[1] Barghlame H, Ferdousi A, Mousavi Ghasemi SA, 2021. Investigation into the behavior of an upgraded section used for Concrete-Filled Steel Tubular Columns (Upgraded CFT) under Cyclic Loading. Journal of Structural and Construction Engineering, vol. 9, p. 86-100. https://doi.org/10.22065/jsce.2021.309337.2601.

[2] Khosravi S, Amirsardari S, Goudarzi MA, 2024. Dynamic Behavior of Rectangular Tanks with Limited Freeboard Under Seismic Loads: Experimental, Analytical and Machine Learning Investigations. Journal of Pressure Vessel Technology, p. 1-34. https://doi.org/10.1115/1.4066967.

[3] Khosravi S, Goudarzi MA, 2023. Seismic risk assessment of on-ground concrete cylindrical water tanks. Innovative Infrastructure Solutions, vol. 8, p. 68. https://doi.org/10.1007/s41062-022-01002-8.

[4] Barmaki S, Sheidaii MR, Azizpour Miandoab O, 2021. Progressive collapse resistance of steel moment frames with different types of beam-to-column welded connections in various column removal scenarios. Journal of Structural and Construction Engineering, vol. 9, p. 59-71. https://doi.org/10.22065/jsce.2021.294557.2492.

[5] Mo J, Uy B, Li D, Thai H-T, Tran H, 2021. A review of the behaviour and design of steel–concrete composite shear walls. Structures, vol. 31, p. 1230-1253. https://doi.org/10.1016/j.istruc.2021.02.041.

[6] Kourehpaz P, Molina Hutt C, Marafi NA, Berman JW, Eberhard MO, 2021. Estimating economic losses of midrise reinforced concrete shear wall buildings in sedimentary basins by combining empirical and simulated seismic hazard characterizations. Earthquake Engineering & Structural Dynamics, vol. 50, p. 26-42. https://doi.org/10.1002/eqe.3325.

[7] Zhang J, Zhao Y, Li X, Li Y, Dong H, 2021. Experimental study on seismic performance of recycled aggregate concrete shear wall with high-strength steel bars. Structures, vol. 33, p. 1457-1472. https://doi.org/10.1016/j.istruc.2021.05.033.

[8] Cook DT, Liel AB, DeBock DJ, Haselton CB, 2021. Benchmarking FEMA P-58 repair costs and unsafe placards for the Northridge Earthquake: Implications for performance-based earthquake engineering. International Journal of Disaster Risk Reduction, vol. 56, p. 102117. https://doi.org/10.1016/j.ijdrr.2021.102117.

[9] Hoult R, Appelle A, Almeida J, Beyer K, 2019. Seismic response of thin, singly reinforced U-shaped walls: Overview and large-scale experimental tests. Proceedings of Concrete, vol. 43, p. 56-69.

[10] Fantilli AP, Ferretti D, Rosati G, 2005. Effect of bar diameter on the behavior of lightly reinforced concrete beams. Journal of Materials in Civil Engineering, vol. 17, p. 10-18. https://doi.org/10.1061/(ASCE)0899-1561(2005)17:1(10).

[11] Oh YH, Han SW, Lee LH, 2002. Effect of boundary element details on the seismic deformation capacity of structural walls. Earthquake Engineering & Structural Dynamics, vol. 31, p. 1583-1602. https://doi.org/10.1002/eqe.177.

[12] Khalfallah S, 2006. Cracking analysis of reinforced concrete tensioned members. Structural Concrete, vol. 7, p. 111-116. https://doi.org/10.1680/stco.2006.7.3.111.

[13] Chrysanidis T, 2014. Size of seismic tensile strain and its influence on the lateral buckling of highly reinforced concrete walls. IOSR Journal of Mechanical and Civil Engineering, vol. 11, p. 18-22.

[14] Esmaeili J, Khoshkanabi SP, Andalibi K, Kasaei J, 2023. An innovative method for improving the cyclic performance of concrete beams retrofitted with prefabricated basalt-textile-reinforced ultra-high performance concrete. Structures, vol. 52, p. 813-823. https://doi.org/10.1016/j.istruc.2023.04.004.

[15] Ghaderi M, Maleki VA, Andalibi K, 2015. Retrofitting of unreinforced masonry walls under blast loading by FRP and spray-on polyurea. Fen Bilimleri Dergisi (CFD), vol. 36, p. 4. https://doi.org/10.17776/CSJ.82511.

[16] Ismaili J, Andalibi K, Kasaei J, 2015. Investigation of the effects of adding nano-alumina on the mechanical properties of concrete. In: 10th International Congress of Civil Engineering, Faculty of Civil Engineering, Tabriz.

[17] Hu H, Wang J, Yan X, 2022. Cracking analysis of members connected by grouted splice sleeves under axial tension. Construction and Building Materials, vol. 322, p. 126487. https://doi.org/10.1016/j.conbuildmat.2022.126487.

[18] Schlicke D, Dorfmann EM, Fehling E, Tue NV, 2021. Calculation of maximum crack width for practical design of reinforced concrete. Civil Engineering Design, vol. 3, p. 45-61. https://doi.org/10.1002/cend.202100004.
[19] Yao G, Xiong X, Ge Y, 2021. Cracking behavior of full-scale pre-tensioned prestressed concrete double-Tee members with steel-wire meshes. Journal of Building Engineering, vol. 44, p. 102658. https://doi.org/10.1016/j.jobe.2021.102658.
[20] Fantilli AP, Mihashi H, Vallini P, 2009. Multiple cracking and strain hardening in fiber-reinforced concrete under uniaxial tension. Cement and Concrete Research, vol. 39, p. 1217-1229. https://doi.org/10.1016/j.cemconres.2009.08.020.
[21] Muhamad R, Ali MM, Oehlers D, Sheikh AH, 2011. Load-slip relationship of tension reinforcement in reinforced concrete members. Engineering Structures, vol. 33, p. 1098-1106. https://doi.org/10.1016/j.engstruct.2010.12.022.
[22] Hong S, Park SK, 2012. Uniaxial bond stress-slip relationship of reinforcing bars in concrete. Advances in Materials Science and Engineering, vol. 2012, p. 1-12. https://doi.org/10.1155/2012/328570.
[23] Tastani S, Pantazopoulou SJ, 2013. Reinforcement and concrete bond: State determination along the development length. Journal of Structural Engineering, vol. 139, p. 1567-1581. https://doi.org/10.1061/(ASCE)ST.1943-541X.0000725.
[24] Naghipour M, Khalili A, Hasani SMR, Nematzadeh M, 2022. Experimental investigation of natural bond behavior in circular CFTs. Steel and Composite Structures, vol. 42, p. 191-207. https://doi.org/10.12989/scs.2022.42.2.191.
[25] Guizani L, Chaallal O, Mousavi SS, 2017. Local bond stress-slip model for reinforced concrete joints and anchorages with moderate confinement. Canadian Journal of Civil Engineering, vol. 44, p. 201-211. https://doi.org/10.1139/cjce-2015-0333.
[26] Bao Y, Lew HS, Sadek F, Main J, 2013. A simple means for reducing the risk of progressive collapse. Concrete International, vol. 35, p. 33-38.
[27] Hussien O, Elafandy T, Abdelrahman A, Abdel Baky S, Nasr E, 2012. Behavior of bonded and unbonded prestressed normal and high strength concrete beams. HBRC Journal, vol. 8, p. 239-251. https://doi.org/10.1016/j.hbrcj.2012.10.008.
[28] Opabola EA, Elwood KJ, 2020. Simplified approaches for estimating yield rotation of reinforced concrete beam-column components. ACI Structural Journal, vol. 117, p. 279-291. https://doi.org/10.14359/51724667.
[29] Belarbi A, 2014. ACI 318-14. Building Code Requirements for Structural Concrete. American Concrete Institute, Farmington Hills.
[30] Pouraminian M, Akbari Baghal AE, Andalibi K, Khosravi F, Arab Maleki V, 2024. Enhancing the pull-out behavior of ribbed steel bars in CNT-modified UHPFRC using recycled steel fibers from waste tires: A multiscale finite element study. Scientific Reports, vol. 14, p. 19939. https://doi.org/10.1038/s41598-024-68682-3.
[31] Mahrenholtz C, Eligehausen R, Hutchinson TC, Hoehler MS, 2017. Behavior of post-installed anchors tested by stepwise increasing cyclic crack protocols. ACI Structural Journal, vol. 114, p. 621. https://doi.org/10.14359/51689023.
[32] Dashti F, Dhakal RP, Pampanin S, 2018. Evolution of out-of-plane deformation and subsequent instability in rectangular RC walls under in-plane cyclic loading: Experimental observation. Earthquake Engineering & Structural Dynamics, vol. 47, p. 2944-2964. https://doi.org/10.1002/eqe.3115.
[33] Dezhdar E, Adebar P, 2015. Estimating seismic demand on concrete shear wall buildings. In: The 11th Canadian Conference on Earthquake Engineering, Canadian Association for Earthquake Engineering, Victoria, BC, Canada.